Journal of Optoelectronics and Advanced Materials Vol. 4, No. 1, March 2002, p. 59 - 66

THE DEFECT CONCENTRATION AND THE ELECTRIC PROPERTIES OF THE UO_2 CERAMIC SAMPLES

G. Chirleşan, D. Chirleşan, S. Anghel, I. Iorga-Simăn

University of Pitesti, Faculty of Sciences, Department of Physics, Tg. din Vale, No. 1, Pitesti 0300, Romania

The correlation between the defect concentration and the electric properties was investigated for UO_2 samples placed in controlled atmosphere. The experimental values of the diffusion coefficient were discussed and interpreted in connection with the increase of the oxygen partial pressure and temperature. The activation energy of the defects was calculated from the variation of the diffusion coefficient.

(Received March 2, 2001; accepted after revision March 4, 2002)

Keywords: UO_2 ceramics, Diffusion coefficient, Defects

1. Introduction

Many researches have been focused on the understanding of the defect diffusion mechanism in solid samples, as well as the effects of the diffusion upon the microstructure and the properties of the materials [1-5]. The defect diffusion produces a series of changes upon the basic material, both at microscopic and macroscopic level. The defects that migrate into a sample initiate a series of microscopic effects (formation of chemical compound, dislocations, clusters, etc.), these effects determine modifications at macroscopic level (corrosion, flow, cracks and fissures, swelling, etc.) [10, 11].

The defect diffusion in ceramic samples is important due to their practical use, such as pellets, fuel cells, probe interfaces. That is why a series of experiments were performed using UO_2 samples, in which the defects diffusion in controlled conditions was monitored [7-9, 19-21].

The modern techniques, recently developed, allowed to perform accurate experiments, which succeeded in emphasizing the influence of the defects and defects' migration upon the inter- and intragranular conductivity.

A series of experiments were carried out on yttria-doped zirconia [12, 13, 18-21]. These experiments demonstrated that the samples Z_F sintered from freeze-dried powders show highest conductivity. A homogeneous microstructure of the ceramics determines an improved conductivity. The intergranular oxygen in conductivity takes place through the clean grain boundary via the same mechanism probably controlled by complex defects.

These results suggested the possibility to use other basic materials in which, by a suitable technological processing, larger and cleaner intergranular surfaces be obtained that determine a significant increase of the ionic conductivity.

For the experiments, UO_2 was selected from the series of tested materials, because a rich volume of technologic knowledge on its processing exists (based on the multiple utilisations of the UO_2 in the nuclear reactors) and because it has the optimal dimensional parameters of the grain structure related to the proposed goal [15,16].

The purpose of the experiments was to analyse the correlation between the defect concentration and the electrical resistance of the samples. The theoretical model based on the theory of diffusion was adapted to the experimental specific conditions, thus resulting the parameters of interest that are to be measured. We have studied the dependence of the ionic conductivity versus temperature and versus oxygen partial pressure

in controlled atmosphere.

2. Theoretical background

The issue of the diffusion process in the context of a defect concentration gradient will be analysed. This will allow to establish the relationship between the electrical conductivity $\sigma(t)$ and the chemical diffusion coefficient D, into a parallelepipedic sample in which the evolution of the electrical resistance versus time will be measured.

Let have H, L and l the dimensions of the sample. Diffusion analysis will be done in the directions x and y. The electric current passes through the sample's volume in the direction x (Fig. 1).

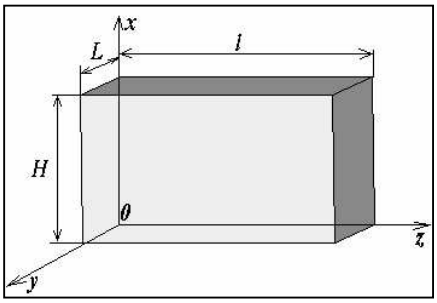

Fig. 1. The model of the investigated amples.

With these hypotheses, Fick's second law will be written as follows:

$$\frac{\partial c}{\partial t} = \overline{D}\left[\frac{\partial^2 c}{\partial x^2} + \frac{\partial^2 c}{\partial y^2}\right] \tag{1}$$

At the moment t, the defects concentration $c(x, y, z)$ in the point (x, y) is a product of functions with a single variable:

$$\begin{gathered} c(x, y, t) = X(x) \cdot Y(y) \cdot Z(z) \\ 0 < x < H \;;\; 0 < y < L \;;\; 0 < z < l \end{gathered} \tag{2}$$

Taking into account this relation, the equation (1) becomes:

$$\frac{1}{T}\frac{dT}{dt} = \frac{\overline{D}}{X}\frac{d^2X}{dx^2} + \frac{\overline{D}}{Y}\frac{d^2Y}{dy^2} \quad - \quad \frac{\overline{D}}{X}\frac{d^2X}{dx^2} = \frac{1}{T}\frac{dT}{dt} - \frac{\overline{D}}{Y}\frac{d^2Y}{dy^2} \tag{3}$$

This equation has to be valid for any x, y and t; therefore, the different functions have to be equal to a constant, thus:

$$\frac{\overline{D}}{X}\frac{d^2X}{dx^2} = -\overline{D}\cdot\lambda^2 \;;\; \frac{\overline{D}}{Y}\frac{d^2y}{dy^2} = -\overline{D}\cdot\mu^2 \tag{4}$$

From the above equation results:

$$\frac{1}{T}\frac{dT}{dt} = -\overline{D}(\lambda^2 + \mu^2) \tag{5}$$

Consequently, the concentration becomes:

$$\begin{gathered} c(x, y, t) = \sum_{m=0}^{\infty}\sum_{n=0}^{\infty}[A_m \sin\lambda_m x + B_m \cos\lambda_m x]\cdot \\ \cdot[C_n \sin\mu_n Y + D_n \cos\mu_n Y]\cdot e^{-\overline{D}(\lambda_m^2 + \mu_n^2)t} + k \end{gathered} \tag{6}$$

The initial and final limit conditions are:

a) $t \to \infty$, $\forall(x,y)$: $c(x, y, t \to \infty) = c_\infty$ (c_∞ is the final concentration of the defects), from where $k = c_\infty$

b) $\forall t \to x = 0$, $\forall y \to c = c_4$ resulting:

$$\sum_{m=0}^{\infty}\sum_{n=0}^{\infty} \cdot B_m [C_n \sin \mu_n Y + D_n \cos \mu_n Y] \cdot e^{-\overline{D}(\lambda^2+\mu^2)t} = 0 \tag{7}$$

and consequently: $B_m = 0$.

Analogous, $\forall t \rightarrow y = 0$, $\forall x \rightarrow c = c_4$ resulting $D_n = 0$.

c) $\forall t$, $\forall y \rightarrow x = H$, $c = c_\infty$ and $\lambda_m = \frac{m\pi}{H}$.

$\forall t$, $\forall x \rightarrow y = L$, $c = c_\infty$ and $\mu_n = \frac{n\pi}{L}$.

d) $t = 0$, $\forall (x, y)$, $c = c_0$ (initial defects concentration). The relation (6) will be written, according to the previous results, as follows:

$$c_0 = c_\infty + \sum_{m=0}\sum_{n=0} A_m \sin\frac{m\pi}{H}x \cdot C_n \sin\frac{n\pi}{L}y \tag{8}$$

By multiplying each member of the equation (8) by the quantity $(\sin p\frac{\pi}{H}x \cdot \sin q\frac{\pi}{L}y)$ and by integrating x from 0 to H and y from 0 to L, it results:

$$\int_0^H \sin\frac{p\pi}{H}x \cdot \sin\frac{m\pi}{h}x dx = \begin{cases} 0 & , m \neq p \\ \frac{H}{2} & , m = p \end{cases} \tag{9}$$

and it one obtains:

$$\frac{H \cdot L(c_0 - c_\infty)}{p\pi \cdot q\pi} \cos\frac{p\pi}{H}x\Big|_H^0 \cdot \cos\frac{q\pi}{L}y\Big|_L^0 = A_p \cdot C_q \cdot \frac{HL}{4} \tag{10}$$

All the terms corresponding to even p and q are zero. For odd p and q, having the form

$$A_p \cdot C_q = \frac{4(c_0 - c_\infty)}{p\pi \cdot q\pi}[1-(-1)^p][1-(-1)^q] \tag{11}$$

$p = 2n + 1$ and $q = 2m + 1$, it is obtained $A_pC_q \neq 0$. From here, it results:

$$c(x, y, t) = c_\infty + \frac{16}{\pi^2}(c_0 - c_\infty)\sum_{m=0}^{\infty}\sum_{n=0}^{\infty}\frac{1}{2n+1}\cdot\frac{1}{2m+1}\cdot$$
$$\cdot \sin(2n+1)\frac{\pi}{H}x \cdot \sin(2m+1)\frac{\pi}{L}y \cdot e^{-\pi^2\overline{D}t\left[\frac{(2n+1)^2}{H^2}+\frac{(2m+1)^2}{L^2}\right]} \tag{12}$$

The measurement of the electric conductivity allows the monitoring of the thermodynamic equilibrium established inside the oxide. If in the crystal, the existence of single type point defects (having the charge ze) is considered, and if the electro-neutrality condition (valid in all the points of the crystal) will be taken into account too, for each moment of time, the following equation can be written:

$$p(x, y, t) = z \cdot c(x, y, t) \tag{13}$$

in which $p(x, y, t)$ and $c(x, y, t)$ represent the void concentration and respectively the point defect concentration, in the point (x, y) at the moment t.

Taking into account that:

$$\sigma = \mu_p \cdot p \cdot e \tag{14}$$

if the variations of the charge mobility μ_p with the concentration will be neglected, on the basis of the former relations, it results that:

$$\sigma(x, y, t) = z \cdot e \cdot \mu_p \cdot c(x, y, t) \tag{15}$$

To determine the electrical conductivity variation with the temperature, the total resistance of the analysed sample has to be measured.

The following relations will be used:

$$\frac{1}{R(t)} = \frac{1}{T}\int_0^H\int_0^L \sigma(x, y, t)\,dx\,dy \tag{16}$$

$$\frac{1}{R(t)} = \frac{z\cdot e\cdot \mu_p}{l}\int_0^H\int_0^L \left\{ c_\infty + \frac{16}{\pi^2}(c_0 - c_\infty)\sum_{m=0}^{\infty}\sum_{n=0}^{\infty}\frac{1}{(2n+1)}\cdot\frac{1}{(2m+1)}\cdot \right.$$
$$\left. \cdot \sin(2n+1)\frac{\pi}{H}x\ \sin(2m+1)\frac{\pi}{L}y\cdot e^{-\pi^2\bar{D}t\left[\frac{(2n+1)^2}{H^2}+\frac{(2m+1)^2}{L^2}\right]} \right\} dx\,dy \tag{17}$$

$$\frac{1}{R(t)} = \frac{L\cdot H}{l}\sigma(t) =$$
$$= \frac{z\cdot e\cdot \mu_p}{l}\left\{ H\cdot L\cdot c_\infty + \frac{64}{\pi^4}H\cdot L(c_0 - c_\infty)\sum_{m=0}^{\infty}\sum_{n=0}^{\infty}\frac{1}{(2n+1)^2}\cdot \right.$$
$$\left. \cdot\frac{1}{(2m+1)^2}\cdot e^{-\pi^2\bar{D}t\left[\frac{(2n+1)^2}{H^2}+\frac{(2M+1)^2}{L^2}\right]} \right\} \tag{18}$$

$$\frac{\sigma(t) - \sigma_\infty}{\sigma_0 - \sigma_\infty} =$$
$$= \frac{64}{\pi^4}\sum_{m=0}^{\infty}\sum_{n=0}^{\infty}\frac{1}{(2n+1)^2}\cdot\frac{1}{(2m+1)^2}\cdot e^{-\pi^2\bar{D}t\left[\frac{(2n+1)^2}{H^2}+\frac{(2m+1)^2}{L^2}\right]} \tag{19}$$

For a time *t* long enough, only the first term of the sum is preserved *(n = m = 0)*, thus:

$$\frac{\sigma(t) - \sigma_\infty}{\sigma_0 - \sigma_\infty} = \frac{64}{\pi^4}e^{-\pi^2\left[\frac{1}{H^2}+\frac{1}{L^2}\right]\bar{D}\cdot t} \tag{20}$$

Taking into account the three dimensions that intervene in diffusion, the defect concentration can be easily deduced:

$$c(x, y, z, t) =$$
$$= c_\infty + \frac{64}{\pi^3}(c_0 - c_\infty)\sum_{m=0}^{\infty}\sum_{n=0}^{\infty}\sum_{p=0}^{\infty}\frac{1}{(2n+1)}\cdot\frac{1}{(2m+1)}\cdot\frac{1}{(2p+1)}\cdot$$
$$\cdot \sin(2n+1)\frac{\pi}{H}x\cdot\sin(2m+1)\frac{\pi}{L}y\cdot\sin(2p+1)\frac{\pi}{l}z\cdot$$
$$\cdot e^{-\pi^2\bar{D}\cdot t\left[\frac{(2n+1)^2}{H^2}+\frac{(2m+1)^2}{L^2}+\frac{(2p+1)^2}{l^2}\right]} \tag{21}$$

and by following a reasoning similar to that one used before for the previous two-dimensional problem, for the three-dimensional case the next result will be obtained:

$$\frac{\sigma(t) - \sigma_\infty}{\sigma_0 - \sigma_\infty} = \frac{64}{\pi^6}e^{-\pi^2\left[\frac{1}{H^2}+\frac{1}{L^2}+\frac{1}{l^2}\right]\bar{D}\cdot t} \tag{22}$$

Having the values of the electrical resistance of the sample from the experimental determinations (and thus, implicitly, its conductivity) at various moments of time, the chemical diffusion coefficient can be calculated by using the equation (22).

3. Experimental

We have designed and used an installation containing the following elements to perform the experiments:

- electric source;
- electric furnace;

- work-vessel;
- monitoring and controlling system of the atmosphere inside the work-vessel;
- electric resistance measuring system.

A sample of UO_2, having the dimensions: L = 9.08 mm; l = 2.5 mm; H = 2.26 mm has been used to carry out the experiments.

For this sample the electric resistance values versus time were monitored, at various temperatures (maintained for a long time, as in the graphics below) and at various partial oxygen pressures.

The temperature's influence was felt by the appearance of a defect concentration gradient, which led to the modification of the sample's electric resistance.

During the experiments the electric resistance of the sample at different times could be measured and from these values, the electric conductivities were calculated.

Having these dependencies, and taking into account the expression between *emf*, E, (the electromotive force) on the two sides of the sample, perpendicular to the diffusion direction, and the oxygen partial pressures on the two sides, whose expression is:

$$E = -\frac{RT}{4F} \cdot \ln \frac{P_{O_2}}{P^0_{O_2}} \tag{23}$$

and also having in mind the relation:

$$\frac{\sigma(t) - \sigma_\infty}{\sigma_0 - \sigma_\infty} = \frac{64}{\pi^6} e^{-\pi^2 \left[\frac{1}{H^2} + \frac{1}{L^2} + \frac{1}{l^2} \right] \overline{D} \cdot t} \tag{24}$$

it was finally possible to deduce the dependence of the diffusion coefficient *D* as a function of the defect concentration gradient in the UO_2 sample.

In the previous relations, the significance of the symbols is:

H, L and *l* represent the height, the width and the length of the parallelepipedic sample;

σ_t is the electric conductivity at the *t* moment;

σ_o is the initial electric conductivity;

σ_∞ is the final electric conductivity, in the new equilibrium conditions;

P_{O2} is the oxygen partial pressure, in equilibrium with the sample, and P^o_{O2} a referential oxygen partial pressure (of the air);

E (mV) is the electromotive force measured at the terminals of the oxygen probe (ZrO_2 yttrium-doped tube).

4. Results and discussion

The measurements were carried out for various temperatures and the results were compared with those of other authors [20, 21].

The chemical diffusion coefficient *D* was determined by measuring the electric conductivity of the sample at different moments of time. The relation (24) was processed by introducing the following notations:

$$\frac{\sigma(t) - \sigma_\infty}{\sigma_0 - \sigma_\infty} = A(t) \tag{25}$$

$$g = -\pi^2 \left[\frac{1}{H^2} + \frac{1}{L^2} + \frac{1}{l^2} \right] \tag{26}$$

It is easy to notice that *g* is a constant depending only on the sample dimensions. The sample used in the experiments had the following dimensions: *L = 9.08 mm; l =2.5 mm; H = 2.26 mm.*

With the above notations, the relation (24) becomes:

$$A(t) = \frac{64}{\pi^6} e^{g \cdot \overline{D} \cdot t} = (ct.)\, e^{g \cdot \overline{D} \cdot t} \tag{27}$$

To calculate the chemical diffusion coefficient, the logarithm function was applied to the expression (27) and then the graphic of the dependence *lnA(t) = f(t)* was drawn.

$$\ln A(t) = (ct.) \cdot g \cdot \bar{D} \cdot t \qquad (28)$$

From the slope of the straight-line (28) the value of the chemical diffusion coefficient was deduced. The graphic representations for various experimental conditions (temperatures and partial oxygen pressures) and also the results of their processing are shown in the next diagrams.

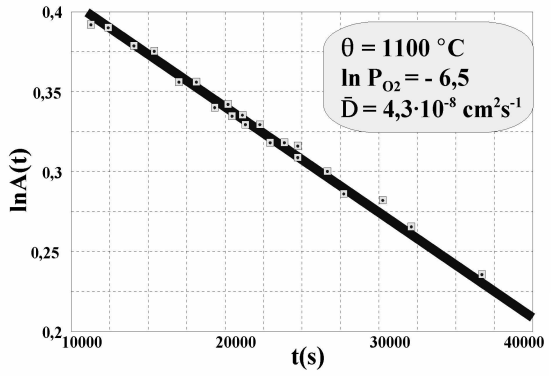

Fig. 2. Dependence of *lnA(t)* versus *t* at 1100°C.

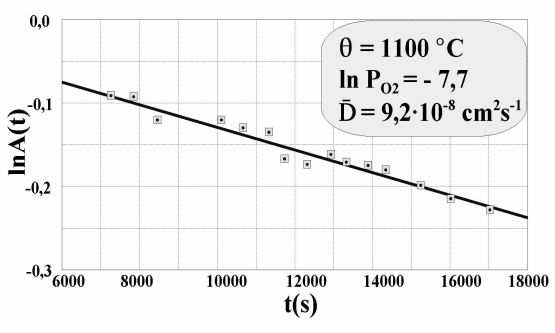

Fig. 3. Dependence of *lnA(t)* versus *t* at 1100°C at another oxygen partial pressure

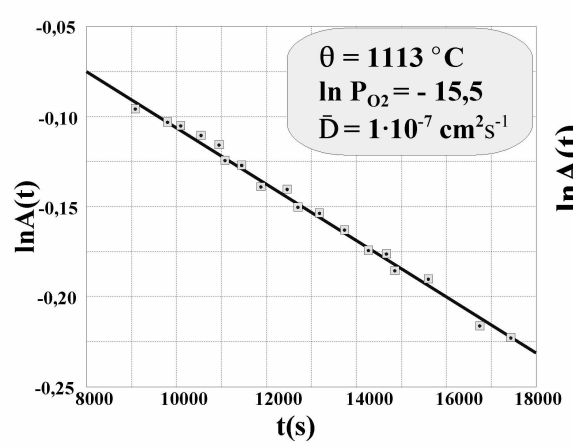

Fig. 4: Dependence of *lnA(t)* versus *t* at 1113°C.

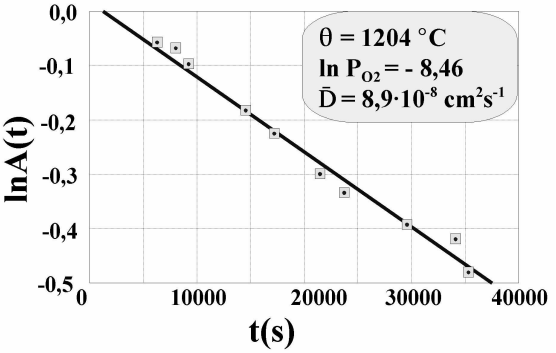

Fig. 5. Dependence of *lnA(t)* versus *t* at 1204°C.

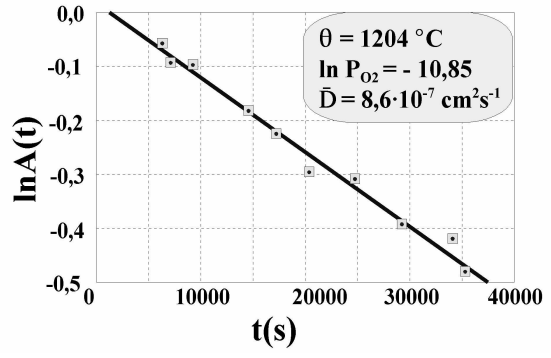

Fig. 6. Dependence of *lnA(t)* versus *t* at 1204°C at another O_2 partial pressure.

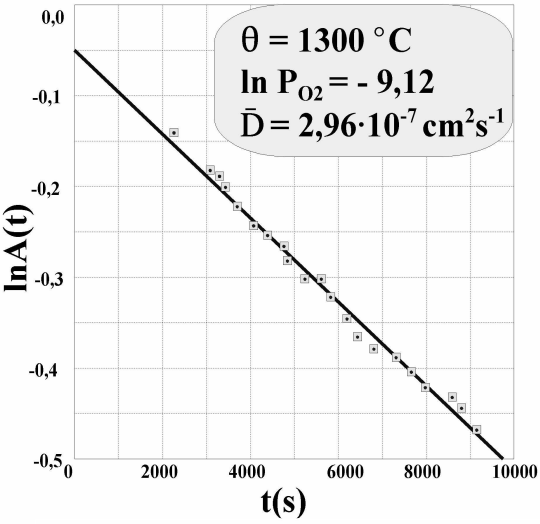

Fig. 7. Dependence of *lnA(t)* versus *t* at 1300°C.

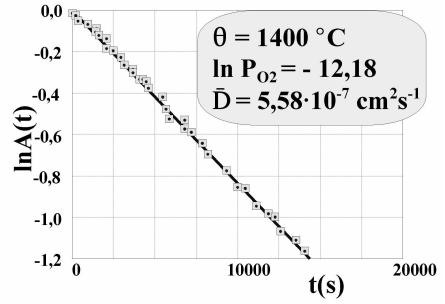

Fig. 8. Dependence of *lnA(t)* versus *t* at 1400°C.

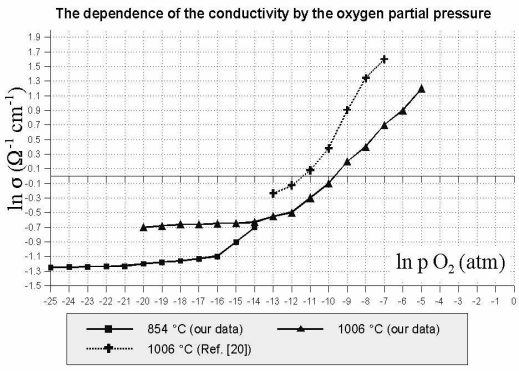

Fig. 9. Dependence of lnσ(t) versus ln P_{O2} at 854°C (original results), 1006°C (original results) and 1006°C (references data).

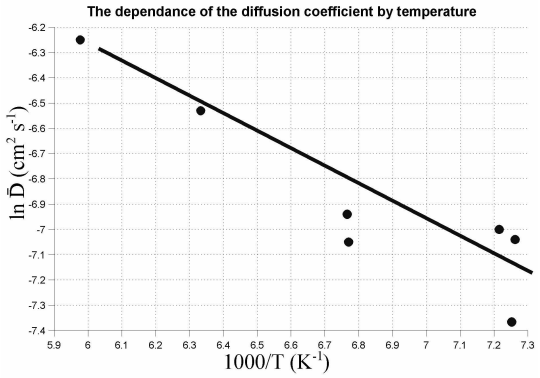

Fig. 10. Dependence of *lnD(t)* versus 1000/T .

The obtained values for the chemical diffusion coefficients, at various temperatures and partial oxygen pressures, were used to determine the activation energy of the defects, according to the relation:

$$E_a = - R \cdot \frac{d(\overline{\ln D})}{d\left(\frac{1}{T}\right)} \tag{29}$$

The value of the activation energy, E_a = 1.36 ± 0.03eV, was obtained from the slope of the Arrhenius type dependence:

$$\ln \tilde{D} = f(10000/T).$$

shown in the Fig. 10. This is in agreement with the results reported by other authors [17, 18, 20, 21].

In these experiments the dependence of the electric conductivity of the stoichiometric UO_2 was followed as function of several factors: temperature, exposure time in controlled atmosphere and the values of the oxygen partial pressure. The experiments led to a set of results in agreement with those reported by other authors [7-11]. It was noticed that the oxygen partial pressure does not significantly influences the time dependence of the electric conductivity of the investigated samples (see the slope of the diagrams in Figs. 3 and 4). Therefore, it seems that the rate of the Frenkel pair formation, like mobile defects of oxygen, is not affected by the increases or decreases of the oxygen partial pressure. On the other hand, the changes in the oxygen partial pressure, at the same temperature, have a major influence upon the chemical diffusion coefficient. The doubling of this coefficient's value is remarkable for a variation with one exponential order in the size of the oxygen partial pressure (as in the diagrams 2 and 3) or even the one order size increasing of the diffusion coefficient with the increasing of the oxygen partial pressure with two exponential orders in its size (diagrams 5 and 6). This fact could be ascribed to the increasing of the oxygen ion mobility, and as a result, to the acceleration of the Frenkel pair formation like oxygen defects. This acceleration is favoured by the increased concentration of the oxygen ions on the first interface of the exposed samples.

These results, although obtained by a totally different experimental pathway, lead to similar

conclusions to those obtained by T. Matsui et al. [17]. The tests were carried out on stoichiometric undoped UO_2 and taking into consideration the results reported by other authors [18], there is a good correlation between them. The results we obtained on undoped UO_2 also fit those obtained in other comparable studies (performed for undoped UO_2 and UO_2 doped with Ti, La, Sc, and Eu [2, 6,14]), in which the temperature at which the slope of the conductivity changes is independent of the kind of dopant and the dopant content, being almost the same to that of undoped UO_2. A good correspondence with other reported results [19] was obtained regarding the transport mechanism, concluding that the intergranular oxide ion conductivity takes place through the clean grain boundary, the mechanism being controlled by the complex defects.

5. Conclusions

The experiments firmly proved the influence of defect concentration gradient and the effects of the defect diffusion on the ionic conductivity of the analysed ceramic samples.

These effects also allowed for the determination of the chemical diffusion coefficient of the sample at various temperatures and partial oxygen pressures. It was thus demonstrated that the increase of the ionic conductivity is due to the intensification of the diffusion process, in various temperature and atmosphere conditions. The obtained results are useful in re-designing the installations for the catalytic treatment of the cars' exhaust gases. Thus, the difference between the partial pressure of the oxygen inside and outside the catalytic installation is the major input factor for the electronic controller of the engine ignition. The results of the present paper might improve the sensibility of this installation, of its main device, which is in fact a ceramic piece, by increasing the activation energy for which the inter-granular ionic conductivity of the oxygen ions occurs. This improvement will be possible by changing the actual type of ceramics with a new one, based on UO_2.

Another direct application of the actual results is the development of solid cells, able to store high quantities of ions such as oxygen, hydrogen and deuterium.

Acknowledgements

We would like to thank Dr. G. Petot-Ervas and Dr. C. Petot (from SPSM laboratory/Ecole Centrale - Paris/France) for their help during the experiments and fruitful advices.

References

[1] C. M. Wayman, Ed. C.C. Koch, Pittsburg, 1985.
[2] T. Matsui, Y. Arita, K. Naito, J. Radioanal. and Nucl. Chem. **143,** 149 (1991).
[3] O. Yamamoto, Y. Takeda, R. Kanno, M. Noda, Sol. State Ion. **22,** 241 (1987).
[4] R. J. Borg, G. J. Dienes, Sol. State Diff., Academic Press, (1988).
[5] T. Inoue, N. Seki, K. Eguchi, H. Arai, J. Electrochem. Soc., **137(8)**, 2523 (1990).
[6] T. Matsui, Y. Arita, K. Naito, Sol. State Ion. **49,** 195 (1991).
[7] H. Solomon, J. Chaumont, C. Dolin, C. Monty, Cer. Trans. **24**, 175 (1991).
[8] R. Dieckmann, Cer. Trans., Am. Cer. Soc. **24,** 49 (1991).
[9] N. Q. Minh, J. Am. Cer. Soc. **76(3)**, 563 (1993).
[10] A. R. Allnatt, A. B. Lidiard, "Atomic transport in Solids", Cambridge University, (1993).
[11] T. Isihara, T. Kudo, H. Matsuda, Y. Takita, J. Am. Cer. Soc. **77(6)**, 1682 (1994).
[12] M. Filal, C. Petot, M. Mokchah, C. Chateau, J. L. Carpentier, Sol. State Ion. **80**, 27 (1995).
[13] C. Petot, G. Petot-Ervas, A. Rizea, Ionics **3**, 405 (1997).
[14] T. Matsui, T. Kawase, K. Naito, J. Nucl. Mater. **186,** 254 (1992).
[15] C. T. Forwood, L. M. Clarebrough, "Electron Microscopy of Interfaces in Metals and Alloys", CSIRO Manufacturing Science and Technology, Australia, (1998).
[16] P. E. J. Flewitt, R. K. Wild, "Physical Methods for Materials Characterisation", UK, (1998).
[17] T. Matsui, Y. Arita and K. Naito, J. Nucl. Mater. **188,** 205 (1992).
[18] T. Matsui, K. Naito, J. Nucl. Mater. **138,** 19 (1986).
[19] A. Rizea, M. Filal, D. Chirleşan, F. Lacour-Laher, C. Petot, G. Petot-Ervas, Ionics **6,** 279 (2000).
[20] N. J. Dudney, R. L. Coble, H. L. Tuller, J. Am. Ceram. Soc. **64,** 627 (1981).
[21] M. Aoki, Y. M. Chiang, I. Kosaki, L. J. Lee, H. L. Tuller, Y. Liu, J. Am. Ceram. Soc. **79**, 1169 (1996).